

decomposition of difluorodiazirine an activation energy of 11 360 cm^{-1} (32.5 kcal/mol) has been determined.² After excitation of the vibrationless S_1 state an excess energy of around 17 000 cm^{-1} (48.7 kcal/mol) is available for dissociation. We calculated the level density at 28 375 cm^{-1} in the ground state and found that it is 2.25×10^5 $1/\text{cm}^{-1}$ (ref 13) using a harmonic approximation. For such high-level densities a complete energy randomization on all vibrational levels should be possible by rapid IVR processes¹⁹ and statistical models should be applicable. From RRKM theory²⁰ we calculate a dissociation rate of 10^{12} s^{-1} for N_2 elimination from difluorodiazirine, which is several orders of magnitude faster than the measured fluorescence decay time, which is on the order of microseconds.¹¹ Therefore we conclude that the measured decay rate is given by the coupling to the electronic ground state and does not merely reflect the RRKM rate for dissociation from the 1A_1 state. Hence, the slow predissociation of F_2CN_2 is due to a weak coupling of the \tilde{A}^1B_1 to the \tilde{X}^1A_1 ground state.

(19) Parmenter, C. S. *Faraday Discuss. Chem. Soc.* 1983, 75, 7.

(20) Marcus, R. A.; Rice, O. K. *J. Phys. Colloid Chem.* 1951, 55, 894.
Marcus, R. A. *J. Chem. Phys.* 1965, 43, 2658.

At present we cannot exclude that there exist other primary reaction steps and N_2 is produced in a secondary reaction. Possible intermediates like linear difluorodiazomethane, F_2CNN , indicated by the formation of tetrafluoro-2,3-diazabuta-1,3-diene, $F_2C=N-N=CF_2$, have been discussed in previous publications.^{2,3,21} Our experiment is not able to detect intermediates. Furthermore, due to the low time resolution of our experiment no information is available on the production rate of N_2 . However, we would like to stress that multiphoton ionization (used in this work) is a suitable method to address this question if combined with a molecular beam experiment. Under collision-free conditions in a molecular beam N_2 could be detected with nanosecond time resolution or better in a pulse-probe experiment.

Acknowledgment. Financial support from the Deutsche Forschungsgemeinschaft and the Fonds der Chemischen Ind. is gratefully acknowledged. H.S. thanks the Hanns-Seidel-Stiftung for a Graduierten Stipendium.

(21) Ogden, P. H.; Mitsch, R. A. *J. Heterocycl. Chem.* 1968, 5, 41.

Oscillations in the $H_2 + Cl_2$ Reaction: Experimental Measurements and Numerical Simulation

D. P. Coppersthaite, J. F. Griffiths,*

School of Chemistry, The University, Leeds, LS2 9JT, U.K.

and B. F. Gray

School of Chemistry, Macquarie University, N.S.W. 2109, Australia (Received: February 19, 1991; In Final Form: April 15, 1991)

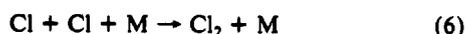
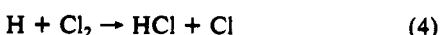
Thermokinetic oscillations during the reaction between hydrogen and chlorine are reported when reaction takes place under semibatch operation. Up to 10 oscillations were observed in a single experiment, and temperature excursions greater than 200 K were measured directly by a thermocouple. The reaction was performed in nonadiabatic conditions by the relatively slow admission of hydrogen to the chlorine already present in the reaction vessel. Total reactant pressures in the range 40–80 Torr were investigated at vessel temperatures between 600 and 650 K. The oscillations were found to exist in a closed region of parameter space determined by the rate of supply of the hydrogen and the vessel temperature. The theoretical background to the existence of the oscillations is derived, and numerical calculations based on established kinetics for the $H_2 + Cl_2$ reaction are presented to relate the experimental observations to these principles. Phase relationships between the molecular reactants, free-radical intermediates, and the reactant temperature are explored.

Introduction

As is documented in chemical kinetic text books, the thermal reaction between hydrogen and chlorine proceeds exothermically according to the overall stoichiometry



from which $\Delta H^\circ_{298} = \Delta U^\circ_{298} = -186 \text{ kJ mol}^{-1}$. The chain propagation may be represented very satisfactorily in its simplest form by the five-step mechanism (eqs 2–5), where M represents



a "chaperone" species. The initiation is known to be sensitive to surface effects.¹ Nevertheless, the above mechanism, or the

analogous model for the $H_2 + Br_2$ reaction, is commonly used as an example for application of the stationary-phase approximation in chemical kinetics. The exothermicity is ignored in such a treatment (i.e., isothermal reaction is assumed), and when the stationary-state approximation is applied to the free radicals H and Cl, the overall reaction rate may be expressed in the form

$$\frac{d[HCl]}{dt} = \frac{-1}{2} \frac{d[H_2]}{dt} = \frac{-1}{2} \frac{d[Cl_2]}{dt} = \frac{k'[H_2][Cl_2]^{1/2}}{\{1 + k''([HCl]/[Cl_2])\}} \quad (7)$$

where k' and k'' represent composites of the elementary rate constants k_2 to k_6 . The retarding effect of HCl becomes prominent at great extents of reaction, but the reaction remains first order with respect to hydrogen throughout and is of order 1/2 with respect to chlorine in the initial stages.

For much of the analysis given below we shall consider only the early stages of the reaction where [HCl] is negligible, and

(1) Noyes, R. M.; Fowler, L. J. *Am. Chem. Soc.* 1951, 73, 3043.

we use a correspondingly simplified form of the rate equation (7). Two quite different time scales must be considered, a fast time scale within which the atomic concentrations themselves change, and a much slower time scale appropriate to the description of the changes in temperature and reactant concentrations. The hydrogen and chlorine atom concentrations attain their stationary-state values on the first time scale, given by

$$\begin{aligned} [H]_s &= (k_3/k_4)[Cl]_s[H_2] \\ [Cl]_s &= (k_2/k_6)^{1/2}[Cl_2]^{1/2} \end{aligned} \quad (8)$$

Both $[H_2]$ and the reactant temperature, encapsulated in the rate constants which appear in eqs 8, vary on the slower timescale, and it is this time scale with which we will be mainly concerned in the present paper.

Spontaneous ignition of $H_2 + Cl_2$ may occur in a closed vessel under nonisothermal conditions in the vessel temperature range 600–700 K, as was shown by Ashmore and co-workers,²⁻⁵ and temperature measurements in the $H_2 + Cl_2$ reaction by use of very fine thermocouples provided some of the earliest direct evidence for self-heating to thermal ignition in gaseous reactions.⁵ The combustion studies show that, for a given composition in a reaction vessel of particular size and shape, there is a quantitatively defined ignition boundary in the pressure-vessel temperature ($p-T_0$) ignition diagram.³ The location of the ignition limit may be predicted satisfactorily by application of thermal ignition theory.⁶ Quasi-stationary-state behavior occurs in the subcritical reaction zone; its theoretical interpretation constitutes a nonlinear problem in at least two variables.^{7,8} The minimum representation involves one reactant concentration and gas temperature.

Our preconceptions as physical chemists may condition us to suppose that the (subcritical) "slow reaction", as opposed to the (supercritical) ignition, constitutes an essentially stable reaction mode. In this paper we show that oscillations are also possible if the traditional experimental procedure of rapid admission of premixed reactants to an evacuated vessel is modified. The procedure that we adopt is the controlled admission of one reaction to a reaction vessel so that it mixes with the other reactant already present in the vessel. This is not a flow system because there is no outflow of reaction products. In chemical engineering terms the system may be classified as a semibatch reactor.

Theoretical Background

If one of the reactants is admitted at an appropriate rate, the system can be described by the following scheme



The overall rate of step b is governed by the form of eq 7 which depends on whether $[X]$ is integrated as $[H_2]$ or $[Cl_2]$, the other component Y being in sufficient excess to give a pseudo-zero-order concentration dependence. Correspondingly, the concentration dependence is either first order or half order with respect to $[X]$. Step b is exothermic and has a significant overall activation energy. By contrast, there is neither heat release nor an activation energy associated with step a in scheme 9. It is simply a constant influx rate.

When there is an overall first-order dependence of rate on reactant concentration, that is when excess chlorine is already in

situ, the scheme 9 is a realization of a thermokinetic oscillator first considered by Sal'nikov⁹ in the 1940s, although the original concept was to explain the origins of oscillatory cool flame phenomena in hydrocarbon oxidation.¹⁰ More extensive analyses were carried out recently by P. Gray and co-workers^{11,12} and, independently, by B. F. Gray and Roberts.¹³ The purpose was to investigate analytically and numerically the properties of two consecutive first-order reactions taking place in a nonadiabatic system, subject to the conditions (i) that all of the heat output was associated with the second reaction, and (ii) that only the second step exhibited a significant temperature dependence (activation energy). As we shall see, the description, and hence the elaboration of the remarkable properties of this thermokinetic model, transposes very satisfactorily to the behavior of an exothermic reaction taking place under semi-batch conditions. Until recently there had been no precedent for experimental test of the theory or indeed recognizable examples of kinetic systems of such a simple kind.^{14,15}

Thus, consider a first-order reaction sequence of the form



taking place in a well-stirred reactor, subject to the conditions $E_a = 0, E_b > 0; \Delta U_a = 0, \Delta U_b < 0$. The conservation equation for the intermediate species X takes the form

$$dx'/dt = k_a a_0 - k_b x' \quad (11)$$

The energy conservation equation takes the form

$$c_v \frac{dT}{dt} = k_b(-\Delta U_b)x' - \frac{\chi S}{V}(T - T_0) \quad (12)$$

In these equations, a and x' represent the species concentrations, k is a rate constant, c_v is a heat capacity per unit volume, ΔU is the internal energy change, χ is a heat-transfer coefficient, S/V represents the surface to volume ratio of the vessel, and $(T - T_0)$ represents the (spatially uniform) temperature excess of the reactants above the temperature of the vessel.

For the purpose of analytical interpretation it is more convenient to cast these equations in a dimensionless form. It is in this respect that the contributions of P. Gray et al.^{11,12} and B. F. Gray and Roberts¹³ differ, although each procedure has its own particular merit and there are common links in the overall conclusions. We base the following summary on the analysis by Gray and Roberts.¹³

Let

$$\begin{aligned} x &= \frac{(-\Delta U_b)R x'}{c_v E_b}, \quad m = \frac{k_a a_0 (-\Delta U_b)R}{c_v E_b Z_b}, \quad \tau = Z_b t, \\ l &= \frac{\chi S}{Z_b c_v V}, \quad u = \frac{RT}{E_b}, \quad u_0 = \frac{RT_0}{E_b} \end{aligned}$$

Z_b is the preexponential factor for reaction b, such that $k_b = Z_b e^{-E_b/RT} = Z_b e^{-(1/u)}$, and is used as the basis for nondimensionalizing the time scale. This yields l as a nondimensionalized cooling parameter, and m as a nondimensionalized parameter to characterize the rate of formation of intermediate X (at a constant concentration of A). The temperature is nondimensionalized by the quotient E_b/R . The expression of m in terms of the initial concentration a_0 is an application of the "pool chemical approximation".¹³

The conservation eqs 11 and 12 take the dimensionless forms

$$dx/d\tau = m - e^{-(1/u)}x \quad (13)$$

$$du/d\tau = e^{-(1/u)}x - l(u - u_0) \quad (14)$$

The stationary states of x and u exist at

(2) Ashmore, P. G.; Norrish, R. G. W. *Proc. R. Soc. London A* 1950, 203, 472.

(3) Ashmore, P. G.; Chanmugam, J. C. *Trans. Faraday Soc.* 1953, 49, 254.

(4) Ashmore, P. G. *Catalysis and Inhibition of Chemical Reactions*; Butterworths: London, 1963.

(5) Ashmore, P. G.; Tyler, B. J.; Wesley, T. A. B. *Tenth Symposium (International) on Combustion*; The Combustion Institute: Pittsburgh, 1965; p 217.

(6) Gray, P.; Lee, P. R. In *Oxidation and Combustion Reviews*; Tipper, C. F. H., Ed.; Elsevier: Amsterdam, 1966; Vol. 2, p 1.

(7) Yang, C. H.; Gray, B. F. *Eleventh Symposium (International) on Combustion*; The Combustion Institute: Pittsburgh, 1967; p 1099.

(8) Gray, B. F. *Trans. Faraday Soc.* 1969, 65, 1603.

(9) Sal'nikov, I. E. *Zh. Fiz. Khim.* 1950, 23, 258.

(10) Minkoff, G. J.; Tipper, C. F. H. *Chemistry of Combustion Reactions*; Butterworths: London, 1962.

(11) Gray, P.; Kay, S. R.; Scott, S. K. *Proc. R. Soc. A* 1988, 416, 321.

(12) Kay, S. R.; Scott, S. K. *Proc. R. Soc. A* 1988, 416, 343.

(13) Gray, B. F.; Roberts, M. J. *Proc. R. Soc. A* 1988, 416, 391.

(14) Griffiths, J. F.; Kay, S. R.; Scott, S. K. *Twenty-second Symposium (International) on Combustion*; The Combustion Institute: Pittsburgh, 1988; p 1597.

(15) Gray, P.; Griffiths, J. F. *Combust. Flame* 1989, 78, 87.

$$x_s = me^{(1/u)}, \quad u_s = u_0 + (m/l) \quad (15)$$

The Hopf curve, which distinguishes the region of instability from that of stability, in the ($u_0 - m$) plane, is defined by the equations

$$\frac{dx}{d\tau} = \frac{du}{d\tau} = \text{tr } J = 0 \quad (16)$$

$$\det J > 0 \quad (17)$$

where $\text{tr } J$ and $\det J$ are the trace and the determinant of the Jacobian matrix from the conservation eqs 13 and 14 at the stationary state. Instability exists when $\text{tr } J > 0$. From 13 and 14

$$J = \begin{vmatrix} -e^{-(1/u_s)} & -(x_s/u_s^2)e^{-(1/u_s)} \\ e^{-(1/u_s)} & (x_s/u_s^2)e^{-(1/u_s)} - l \end{vmatrix} \quad (18)$$

from which

$$\det J = le^{-(1/u_s)} \quad (19)$$

$$\text{tr } J = -l - e^{-(1/u_s)} + (x_s/u_s^2)e^{-(1/u_s)} \quad (20)$$

The application of condition (16) and elimination of x_s by use of the stationary-state solutions 15 yields

$$u_0 = u_s - (u_s^2/l)(e^{-(1/u_s)} + l) \quad (21)$$

$$m = u_s^2(e^{-(1/u_s)} + l) \quad (22)$$

These solutions define the locus of the Hopf surface in the ($u_0 - m - l$) three-dimensional space. Thus the locus of the Hopf curve in the ($u_0 - m$) plane represents a section in space defined at a given value of l . Since u_0 is only single valued in m , each Hopf curve is derived conveniently from the solutions 21 and 22 by first solving for u_s at given m , and then by determining the corresponding u_0 from u_s (where $u_0 = u_s - (m/l)$). Retracing our steps to the dimensional terms, we see that at a given heat-transfer coefficient, represented by l , the relationship between the rate of formation of X, represented by m , and the ambient temperature, in dimensionless form as u_0 , determines whether or not the system is stable. The nature of the unstable solution is such that the time-dependent behavior would be observed as indefinite oscillations in reactant temperature and concentration of the intermediate species X. The stable solutions that lie outside but close to the Hopf boundary are found to be stable foci.¹¹⁻¹³ This means that damped oscillations must take place during the transient approach to the stable states $[X]_s, T_s$.

Relationship to the Semibatch Reactor and Numerical Analysis

The stationary-state solutions (x_s, u_s) are determined on the assumption that the concentration of A does not change. Following scheme 9, if step a represents the constant supply of a reactant to the vessel, the problem is then presented as a supply of reactant at a rate characterized by the product $k_a a_0$ (or m in dimensionless terms) into a reactor at temperature T_0 (or u_0 in dimensionless terms). The chemistry is represented solely by step b, and what is described above as "the concentration of the intermediate X" becomes the concentration of the reactant A in the reaction vessel. The stationary-state solutions become exact solutions to the conservation equations, a pseudo-zero-order dependence with respect to Y being assumed. If the extent of consumption of reactant Y in step b is significant then unstable, oscillations cannot be sustained indefinitely, and a supplementary consequence is that the pseudo-first-order rate constant $k_b[Y]$, from (9), falls as the reactant Y is consumed. These features become evident in the numerical analysis.

The formal analytical treatment applies to step b as a first-order exothermic reaction. While the criteria that the reaction is exothermic and exhibits an activation energy are prerequisites, it seems most likely that the points of principle discussed here are applicable to reactions of more complex overall order. Although, in general, numerical solutions may have to be sought for the criteria for stability of more complex systems, a similar analysis

can be carried out with the equations for half-order concentration dependence and similar quantitative conclusions can be reached.¹⁶

In either case some interesting deductions can be made from the "steady-state" expressions for $[H]$ and $[Cl]$. We shall consider only the case of a first-order reaction, i.e., the influx of H₂. The expressions 8 can be rewritten

$$[H]_s = \frac{k_3 k_2^{1/2} [H_2]}{k_4 k_6^{1/2}}$$

$$[Cl]_s = (k_2/k_6)^{1/2} [Cl_2]^{1/2} \quad (23)$$

On differentiating each of these with respect to the slow time and remembering that k_2, k_3, k_4 , and k_5 are functions of temperature, which is itself varying on the slow time scale, we obtain

$$\frac{d[Cl]_s}{dt} = (k_2/k_6)^{1/2} [Cl_2]^{1/2} \frac{E_2}{2RT} \frac{dT}{dt} \quad (24)$$

From this expression it is obvious that the chlorine atom concentration and the reactant temperature would be expected to be in phase during the oscillations. A similar treatment of $[H]_s$ in eq 23 does not give an equally simple prediction because the concentration of H₂ in the reactor also oscillates on the slow time scale. Only a finite number of oscillations can take place because the chlorine is eventually completely consumed. A computational treatment of the thermokinetic equations to represent the H₂ + Cl₂ reaction, which is given below, confirms these results. Experimental verification of the phase relationships has not yet been established.

The numerical analysis of the thermokinetic interactions in the hydrogen + chlorine reaction under a semibatch mode of operation was based on the integration of the differential equations representing the mass conservation of the species H₂, Cl₂, HCl, H, and Cl in each elementary reaction (2)–(6) and the inflow of the H₂ to the vessel. The energy conservation was expressed in terms of the rates of heat release from each step, derived from the product of ΔU and instantaneous rate, and the heat loss to the vessel walls, derived from a measured, Newtonian heat-transfer time. The reactant flow under semibatch conditions to achieve a constant supply rate throughout the chemical period was determined from the measured, characteristic flow time through an entry port to the vessel. Spatial uniformity of temperature and concentration were assumed. The numerical methods, which make use of the SPRINT integration package,¹⁷ have been discussed in detail elsewhere.^{18,19}

Apparatus and Experimental Methods

The reaction was carried out in a spherical Pyrex glass vessel (2.0 dm³) which was connected to a vacuum line. There were independent storage reservoirs for the chlorine and hydrogen. The chlorine was admitted to the reaction vessel to a known initial pressure, as measured by a manometer. The hydrogen was maintained at a sufficiently high excess pressure in a large bulb (5.0 dm³) to ensure that, when it was admitted to the reaction vessel at a controlled rate via a capillary tube, a virtually constant supply rate was maintained until at least an equal pressure of hydrogen to that of chlorine had entered the vessel. The rate of entry was calibrated from the pressure record obtained from the flow of hydrogen into nitrogen at the same pressure as the chlorine in the vessel, so that direct contact between chlorine and the pressure transducer was avoided. The capillary (0.3 mm diameter \times 35 mm long) was mounted horizontally within the reaction vessel with its tip at ca. 40 mm from the wall. The capillary was connected to a flow tube which entered the vessel via a side arm located at the central plane of the vessel.

(16) Gray, B. F.; Thuraisingham, R. Unpublished results.

(17) Berzins, M.; Furzeland, R. M. TNER 85058, Shell Research Ltd., 1985.

(18) Baulch, D. L.; Griffiths, J. F.; Pappin, A. J.; Sykes, A. F. *Combust. Flame* 1989, 73, 87.

(19) Griffiths, J. F.; Sykes, A. F. *Proc. R. Soc. A* 1989, 422, 289.

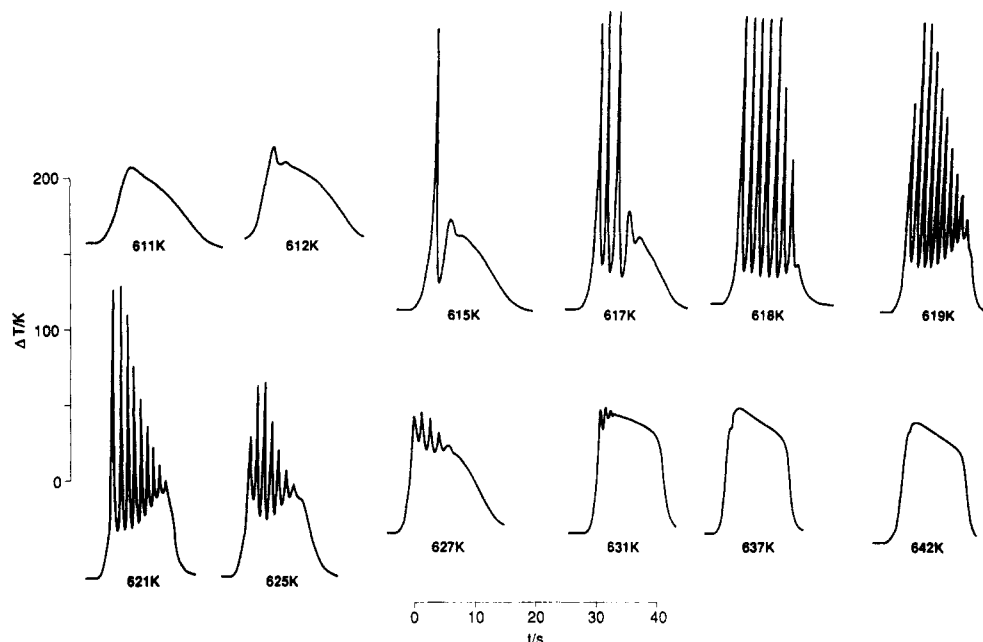


Figure 1. ΔT -time records for a series of experiments over a range of vessel temperatures, as indicated. The initial partial pressure of chlorine was 40 Torr. The rate of pressure change resulting from the admission of hydrogen was 0.6 Torr s^{-1} .

The reaction vessel was located in a recirculating air oven in order to maintain a uniform surface temperature ($\pm 1 \text{ K}$). The temperature excess within the reactants was monitored by a Pt-Pt/13% Rh thermocouple ($25 \mu\text{m}$ diameter wire, silica coated) by reference to a similar junction attached to the external surface of the reaction vessel. The internal junction was located close to the center of the vessel. The signal was recorded either on a chart recorder or on an oscilloscope. A supplementary thermocouple pair (chromel/alumel), with its reference junction in ice, was used to measure the oven temperature.

The initial pressure of chlorine in each experiment was 40 Torr. The external pressures of hydrogen in the reservoir were varied over the range 300–600 Torr. Typical rates of pressure change on admission of hydrogen were 0.5 – 1.0 Torr s^{-1} , thus giving a time for complete reaction of 40–80 s (eq 1). The diffusion rate of hydrogen was sufficiently fast at the experimental pressure that, on entry, it was regarded to be well-distributed throughout the vessel. However, in the absence of forced convection,^{14,15} spatially nonuniform temperatures developed as a consequence of exothermic reaction, and so the measured temperature excess did not constitute a fully quantitative record of the events taking place.

The stirred, closed vessel used in previous work^{14,15,20} contained a stainless steel rotor. We had hoped to obtain experimental results in the present work that were in close quantitative accord with the theoretical interpretation by use of this system. However, the results of initial experiments revealed such a marked catalytic activity at the stirrer surface that we were unable to achieve satisfactory reproducibility.

The vessel temperature was varied in the range 600–650 K. The overall pattern of behavior was thus mapped as a function of the vessel temperature and reactant supply rate, i.e., in the u_0 - m plane as set out in the Theoretical Background section. The Newtonian cooling time, and from it the overall heat-transfer coefficient, was determined in supplementary experiments from the cooling rate following thermal ignition of hydrogen + chlorine mixtures.

Results

(a) Experiment. The thermocouple records from successive experiments when hydrogen was admitted to the chlorine at vessel temperatures in the range 610–640 K are shown in Figure 1. The supply rate of hydrogen to the reaction vessel was 0.6 Torr s^{-1} ,

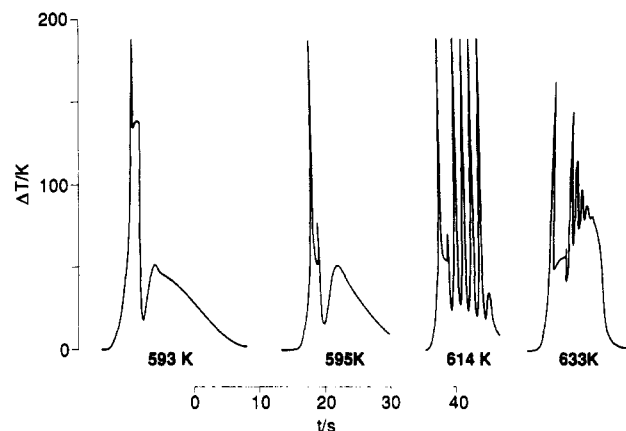


Figure 2. ΔT -time records for a series of experiments as in Figure 1. The rate of pressure change resulting from the admission of hydrogen was 1.2 Torr s^{-1} .

which corresponds to $0.015 \text{ mol m}^{-3} \text{ s}^{-1}$ at 620 K. At the lowest vessel temperatures, there was an initial rise in temperature excess within the reactants to reach a maximum of approximately 30 K after ca. 10 s from the start of reaction. There was then a slow decline as the chlorine was gradually consumed. Repetition of this experiment at a slightly higher vessel temperature gave a very similar result, but we note a vestigial oscillation in the vicinity of the temperature maximum. A further increase of the vessel temperature caused the onset of dramatic oscillations, with a single, large pulse being observed at 615 K. Ten oscillations occurred at 619 K. The recorded temperature rise exceeded 200 K in the largest excursions. As is seen in Figure 1, the large-amplitude oscillations become increasingly damped as the vessel temperature is raised. At its shortest, the period of oscillations was ca. 1.5 s. No oscillations occurred at vessel temperatures in excess of 638 K at the particular supply rate of this series of experiments. The maximum temperature excess in the nonoscillatory reaction that occurred at $T_0 > 638 \text{ K}$ was reached rapidly and it exceeded 50 K.

Rather similar families of results were obtained at different supply rates of hydrogen in the range 0.5 – 1.0 Torr s^{-1} , corresponding to the range of external pressures of hydrogen of 300–600 Torr. However, additional complexities were observed in the temperature record at higher hydrogen flow rates (Figure 2). The oscillations existed in a closed region of parameter space deter-

(20) Griffiths, J. F.; Gray, B. F.; Gray, P. *Thirteenth Symposium (International) on Combustion*; The Combustion Institute: Pittsburgh, 1971; p 239.

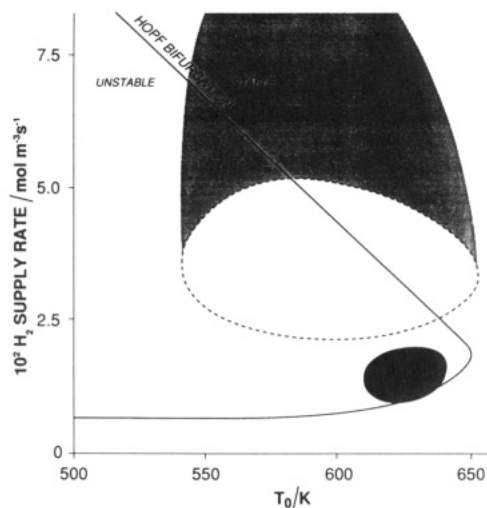


Figure 3. Parameter space in which oscillations were located experimentally (heavy shading) and calculated numerically (broken line) expressed in terms of the H₂ supply rate and the vessel temperature. The light shading represents the region in which phenomena of the kind displayed in the inset of Figure 4 were predicted to occur (see text). The locus of the Hopf bifurcation (eqs 21 and 22) is also shown.

TABLE I: Kinetic and Thermochemical Data for Simulation of the Experimental Results

reaction	A factor	E/ kJ mol ⁻¹	ΔU ^o ₂₉₈ / kJ mol ⁻¹	ref
1	6 × 10 ⁻³ s ⁻¹			
2	1 × 10 ¹¹ mol ⁻¹ m ³ s ⁻¹	182.9	245	
3	1 × 10 ⁶ mol ⁻¹ m ³ s ⁻¹	23.0	3	21, 22
4	8 × 10 ⁷ mol ⁻¹ m ³ s ⁻¹	0.6	-189	22, 23
5	5 × 10 ⁶ mol ⁻¹ m ³ s ⁻¹	1.7	-3	22
6	1 × 10 ⁵ mol ⁻² m ⁶ s ⁻¹	0	-245	22, 24

χS/V = 150 W m⁻² K⁻¹

mined by rate of supply of hydrogen and the vessel temperature, as shown in Figure 3. The principal characteristics within the unstable region are (i) to the left-hand side, the existence of one large temperature excursion, as observed at 615 K in Figure 1, (ii) in the center, the existence of predominantly undamped oscillations, as observed at 618 K in Figure 1, and (iii) to the right-hand side, the existence of damped oscillations.

The extent of the temperature range over which the thermokinetic oscillations existed was reasonably reproducible, although from day-to-day there could be shifts of 5–10 K in the lowest vessel temperature at which oscillations occurred. This was probably a consequence of surface activity, and although a rigorous experimental procedure was adopted we did not find a way of eliminating this variation. The homogeneous control of initiation and termination by nitric oxide, as used by Ashmore and Chanmugam³ in their thermal ignition studies, could have been one possibility, but the additional complexity of the present experiments made its inclusion in the reactant mixture more difficult.

(b) Numerical Model. The thermochemical and kinetic parameters, and the heat-transfer and flow characteristics that were used in the numerical modeling, are given in Table I. Literature values of kinetic data for the propagation steps 3–5 were used in the computations with only minor modification. However, in order to simulate oscillatory reaction within the experimental temperature range the parameters of the rate controlling step 3 had to be set close to those given by Fettis and Knox²¹ rather than at the values recommended by Baulch et al.²²

(21) Fettis, G. C.; Knox, J. H. *Prog. React. Kinet.* 1964, 2, 1.

(22) Baulch, D. L.; Duxbury, J.; Grant, S. J.; Montague, D. C. *Evaluated Data for High Temperature Reactions. J. Phys. Chem. Ref. Data* 1981, 4, Suppl. 1, 10.

(23) Bernard, P. P.; Clyne, M. A. A. *J. Chem. Soc. Faraday Trans. 2* 1977, 73, 298.

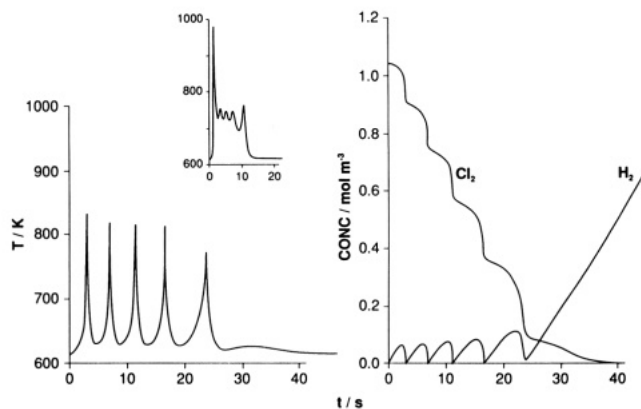


Figure 4. Numerical computations of the temperature and concentration-time records for Cl₂ and H₂ simulated at a vessel temperature of 600 K and initial chlorine partial pressure of 40 Torr. The inflow rate of hydrogen is 0.03 mol m⁻³ s⁻¹. A temperature record at double the inflow rate is shown in the inset.

The choice of the initiation and termination rate parameters presented particular difficulties. When values of the Arrhenius parameters for homogeneous initiation (2) were taken, the reactivity of the computed results was so low that negligible rates and extents of reaction were predicted at conditions corresponding to the experimental range. We attribute this discrepancy to surface activity in the experiments giving heterogeneous initiation.^{1,3} Also, in numerical tests of the isothermal reaction between hydrogen and chlorine in a closed vessel at 600 K, the termination rate constant by Bader and Ogryzlo²⁴ was far too low to permit a stationary state of Cl and H atoms to be attained in a reasonable time.

In view of these inconsistencies, we investigated the numerical solutions to eq 9 under conditions simulating the experimental reactant concentrations, inflow rates, and vessel temperatures to establish appropriate values for Z₂, E₂/R, and Z₆. The most satisfactory location of the oscillatory region was obtained by E_b/R = 13 800 K and Z_b = 1 × 10⁹ s⁻¹, but only at "hydrogen supply rates" in excess of 0.02 mol m⁻³ s⁻¹. A stationary-state analysis of the kinetic scheme in the absence of retardation by HCl yields

$$Z_b = Z_3(Z_2/Z_6)^{1/2}[Cl_2]_0^{1/2}, \quad E_b/R = (E_3 + E_2/2 + E_6/2)/R$$

from which the Arrhenius parameters for reactions 2 and 6 were then derived (Table I). The temperature coefficient for (2) seems plausible if surface activity plays a part. The anomalous value for Z₂, which may be similarly explained, originates in the numerical analysis from the ratio Z₂/Z₆ and constraints on Z₆ set by the need to establish a stationary state within a short reaction time.

A simulation of temperature oscillations is shown in Figure 4. This represents the reactant temperature, no correction being made for the response of the thermocouple as would be required to represent the experimental measurements.¹⁸ Temperature rises in excess of 200 K are predicted in the successive oscillations. The corresponding simulations of the reactant concentrations show how the extent of reaction of chlorine at each oscillation is linked to the inflowing concentration of hydrogen and its accelerated consumption as the temperature increases (Figure 4). The curtailment of the sustained oscillations by the complete consumption of chlorine and the linear rise in hydrogen concentration subsequent to the completion of chemical reaction is clearly seen. In highly damped oscillations the pattern of the predicted behavior is very similar in kind, but the oscillatory reaction ceases before all of the chlorine has been consumed. The initial temperature peak prior to the onset of oscillations in Figure 2 may also be identified in the numerical computations at higher inflow rates of hydrogen (e.g., inset in Figure 4). Under nonoscillatory con-

(24) Bader, L. W.; Ogryzlo, E. A. *Nature* 1964, 201, 492.

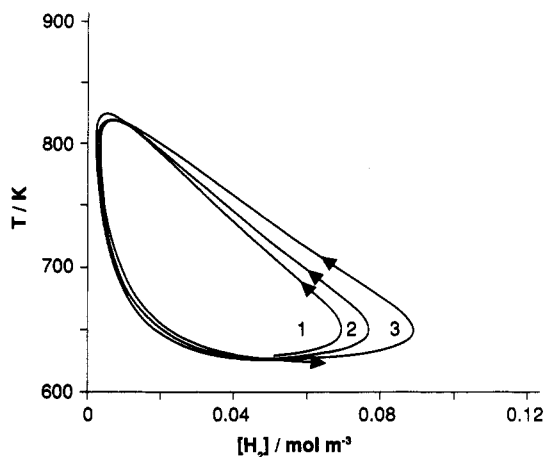


Figure 5. Phase map of the H_2 concentration in the vessel versus the simultaneous reactant temperature T during the three intermediate oscillations shown in Figure 4. The arrows indicate the direction of motion; $[\text{H}_2]$ reaches its maximum before that of T in each cycle.

ditions there is a monotonic decay in chlorine concentration throughout reaction. Spatially uniform concentrations and temperatures were assumed in the numerical analysis, and so fully quantitative accord cannot be expected between the experimental and numerical results.

The region of the $(T_0$ -flow) parameter space in which oscillations are predicted from the full kinetic models is shown in Figure 3. It is displaced from and it is more extensive than the experimentally measured region. These discrepancies may arise mainly from the failure of natural convection and diffusion to achieve spatial uniformity of temperature and concentration in the experiment. Nevertheless, the prediction of oscillations in a spatially uniform environment testifies to the thermokinetic origins of the experimental observations, rather than as artifacts of convection or poor mixing. The additional shaded area above the closed region of the numerical analyses represents the results of the kind shown in the inset of Figure 4. In formal terms represented by (9), this more complex pattern originates from the reduction of Z_b which is caused by the decay of the chlorine concentration.

The locus of the Hopf bifurcation (eqs 21 and 22) at $l = 5 \times 10^{-9}$, corresponding to $\chi S/V = 150 \text{ W m}^{-3} \text{ K}^{-1}$, encompasses the experimental conditions at which oscillations occurred. The locus also bisects the zone in which numerical oscillatory solutions were obtained, confirming that, in the absence of continuous flow, it becomes difficult to distinguish sustained oscillations from the transient, damped oscillatory approach to the stable stationary state when reactant consumption takes place.

Discussion

It is extremely difficult to obtain close quantitative agreement between the experimental observations and the morphology in a two-dimensional plane mapped from numerical predictions. Often, abbreviated kinetic schemes²⁵ or simple formal structures²⁶ are more successful in their own way than the exploitation of very detailed kinetic models. However, numerical modeling, when found to give a satisfactory representation of the experimental measurements, opens up opportunities for analysis that would not be readily accessible by experimental methods. The present study shows what can be achieved when a generally accepted, and relatively simple, kinetic model is used to interpret the nonlinear response of a nonisothermal system.

Phase differences exist between at least two of the independent variables when oscillations occur. The phase relationship between T and $[\text{H}_2]$ (Figure 5) matches the time-dependent behavior of Figure 4 and is plotted over the three intermediate oscillations.

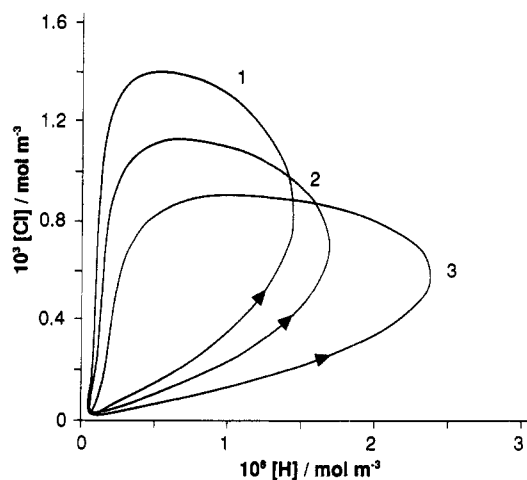


Figure 6. Phase map of the H atom concentration in the vessel versus the simultaneous chlorine atom concentration during the three intermediate oscillations shown in Figure 4. The arrows indicate the direction of motion; $[\text{H}]$ reaches its maximum before that of $[\text{Cl}]$ in each cycle.

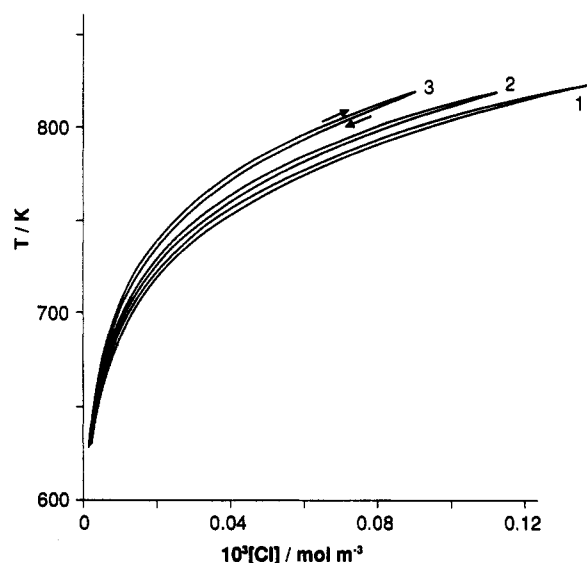


Figure 7. Phase map of the Cl atom concentration in the vessel versus the simultaneous reactant temperature during the three intermediate oscillations shown in Figure 4. The arrows indicate the direction of motion; $[\text{Cl}]$ reaches its maximum simultaneously with T in each cycle.

The limit cycles confirm the theoretical foundation and show that the concentration of molecular hydrogen in the vessel reaches its peak in each cycle before the peak is reached in the reactant temperature. The time difference is approximately 0.82 s. In order to make the same measurement experimentally, which could be achieved by continuous monitoring of the hydrogen concentration by mass spectrometry, it would be essential to ensure either well-matched instrumental responses or accurate corrections to them in order to be able to relate the concentration and thermal records in a fundamental way.

When the concentrations of the hydrogen and chlorine atoms are taken from the same results output and their instantaneous concentrations are plotted in a phase plane, the limit cycles show that the H atom concentration has passed through its maximum and is declining at the point where the Cl atom concentration is at its peak (Figure 6). The time difference between these maxima that is derived numerically is 54 ms. The chlorine atom concentration is plotted versus the instantaneous reactant temperature in Figure 7. These variables reach their maxima simultaneously in each cycle, which signifies that $[\text{Cl}]$ is in phase with the temperature rise, as predicted by eq 24. The pronounced curvature of each loop in this particular phase map arises because the constant of proportionality in (24) is itself nonlinearly dependent on the prevailing temperature as a result of the high activation

(25) Field, R. J. In *Oscillations and Traveling Waves in Chemical Systems*; Field, R. J., Burger, M., Eds.; Wiley: New York, 1985; Chapter 2, p 55.

(26) Wang, X. J.; Mou, C. Y. *J. Chem. Phys.* **1985**, *83*, 4554.

energy for the decomposition of Cl_2 (reaction 2).

Although most systems are considerably more complex in kinetic terms than the consecutive first-order reactions invoked in the Sal'nikov scheme, there is no doubt that it represents the simplest possible formal structure that is capable of exhibiting thermokinetic oscillations. The thermokinetic interactions of the $\text{H}_2 + \text{Cl}_2$ reaction under semibatch conditions in a nonadiabatic reactor are fully represented by a two-dimensional model in which the independent variables are a reactant concentration (H_2) and the reactant temperature (T). An essential ingredient of all such systems is that thermal feedback should take place, just as is required for "classical" thermal ignition. Thermal ignition itself is characterized by two time scales, that for the chemical process (which is temperature dependent and responds to the thermal feedback) and that for the heat loss processes (such as the Newtonian or Fourier time scales). In addition to these two time

scales, the Sal'nikov system is characterized by a third, independent parameter, namely the time scale for the first step ($=1/k_1$). These three time scales, coupled to the thermal feedback, constitute the minimum requirement for the existence of thermokinetic oscillations.

We close on an important practical point of safety in chemical reactors that emerges from both the theory and the experiments. In general, the expedient to increased safety of operation would be appear to reduce the temperature of the system. Under semibatch operation, the reduction of reactor temperature could lead to violent oscillations in an exothermic reaction with potentially damaging or hazardous consequences.

Acknowledgment. We thank SERC for a Visiting Fellowship (B.F.G.).

Registry No. H_2 , 1333-74-0; Cl_2 , 7782-50-5.

Flow-Tube Kinetics Study of the Reaction between Ground-State Hydrogen Atoms and Nitromethane

Taeho Ko, William F. Flaherty, and Arthur Fontijn*

High-Temperature Reaction Kinetics Laboratory, The Isermann Department of Chemical Engineering, Rensselaer Polytechnic Institute, Troy, New York 12180-3590 (Received: February 22, 1991; In Final Form: April 25, 1991)

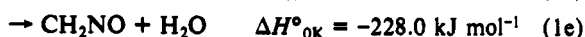
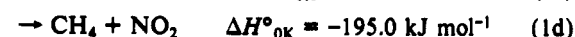
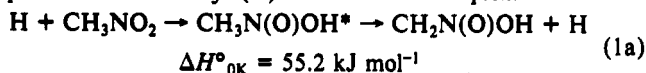
The kinetics of the $\text{H} + \text{CH}_3\text{NO}_2$ reaction have been studied by using a discharge-flow resonance-fluorescence technique. H atoms are produced from microwave discharges through NH_3/Ar mixtures. The data in the 360–570 K range are well fitted by the empirical expression $k(T) = 7.8 \times 10^{-12} \exp(-1878K/T) \text{ cm}^3 \text{ molecule}^{-1} \text{ s}^{-1}$. Precision of the data varies from ± 6 to $\pm 11\%$, and the resulting accuracy is estimated to be better than $\pm 20\%$, where both figures represent 2σ statistical confidence intervals. Results of some experiments where H_2 was discharged indicate that the channel leading to OH and CH_3NO is significant for the reaction. A comparison of the kinetics of several reactions where a methyl-group hydrogen is abstracted by H atoms indicates that such a channel is not important in the present work but could become significant at elevated temperatures. To confirm the accuracy achieved with the present apparatus, measurements on the $\text{H} + \text{C}_6\text{H}_6$ reaction have been made in the 410–530 K range and are compared to results from other studies.

Introduction

In nitramine propellants combustion, the reactions of H atoms with the nitro group play a role. To help elucidate the chemistry of nitramine propellant combustion, we have previously studied the kinetics of the $\text{H} + \text{NO}_2$ reaction.¹ In the present communication, the results of a study of the reaction



are reported. In an abstract, Slemr and Warneck² give $k_1(T) = 2.7 \times 10^{-12} \exp(-1761K/T) \text{ cm}^3 \text{ molecule}^{-1} \text{ s}^{-1}$ for the 298–398 K range, which appears to represent the only previous rate coefficient measurements. However, several mechanistic studies have been made. Melius calculated the energetics of the reaction paths using the BAC-MP4 method and suggested that the reaction proceeds via an $\text{CH}_3\text{N}(\text{O})\text{OH}^*$ addition complex:³



In a crossed molecular beam study, Dagdigian and co-workers have observed OH signals in the reaction between H and CH_3NO_2 and concluded that the $\text{OH} + \text{CH}_3\text{NO}$ channel is significant.⁴

The present study was undertaken to expand the temperature range of the rate coefficient measurements and assess the significance of the OH production channel (1b) under thermal (bulk) reaction conditions. While our earlier studies of H-atom reactions,^{1,5} including the $\text{H} + \text{NO}_2$ measurements,¹ were made by using the HTP (high-temperature photochemistry) technique, this approach was judged unsuitable for the present work, since the flash lamp required for photolytic H-atom production from CH_4 ¹ or NH_3 ⁵ will generate NO_2 ,⁶ which is only weakly bonded ($\approx 250 \text{ kJ mol}^{-1}$)⁷ to the CH_3 group. As the measured¹ rate coefficients for the $\text{H} + \text{NO}_2$ reaction are $> 1 \times 10^{-10} \text{ cm}^3 \text{ molecule}^{-1} \text{ s}^{-1}$, i.e., about 10^4 times greater than the values reported² for reaction 1, the dissociation of the C–N bond would result in overestimation

(3) (a) Melius, C. F. *J. Physique. Coll. C4*. 1987, 48, 341. (b) Melius, C. F., private communications, Dec 1990.

(4) Dagdigian, P. J. In *Combustion Probes for Solid Nitramines*; Shaw, R. W., Johnston, S. C., Adams, G. F., Eds.; Report of the Workshop held in Livermore, CA, June 9–11, 1986. Miziolek, A. W.; Melius, C. F.; Thorne, L. R.; Dagdigian, P. J.; Alexander, M. H. *Gas Phase Combustion Chemistry of Nitramine Propellants*; Ballistics Research Laboratory Technical Report BRL-TR-2906, March 1988.

(5) Ko, T.; Marshall, P.; Fontijn, A. *J. Phys. Chem.* 1990, 94, 1401. Marshall, P.; Ko, T.; Fontijn, A. *J. Phys. Chem.* 1989, 93, 1922.

(6) Taylor, W. D.; Allston, T. D.; Moscato, M. J.; Fazekas, G. B.; Kozlowski, R.; Takacs, G. A. *Int. J. Chem. Kinet.* 1980, 12, 231.

(7) McKee, M. L. *Chem. Phys. Lett.* 1989, 164, 520.

(1) Ko, T.; Fontijn, A. *J. Phys. Chem.* 1991, 95, 3984.

(2) Slemr, F.; Warneck, P. *Ber. Bunsen-Ges. Phys. Chem.* 1975, 79, 1163.